# Photo-Cross-Linkable PNIPAAm Copolymers. 4. Effects of Copolymerization and Cross-Linking on the Volume-Phase Transition in Constrained Hydrogel Layers

Marianne E. Harmon,[†] Dirk Kuckling,*[,†,‡] Pradeep Pareek,[‡] and Curtis W. Frank*[,†]

*Department of Chemical Engineering, Stanford University, Stanford, California 94305-5025, and Institut für Makromolekulare Chemie und Textilchemie, Technische Universität Dresden, D-01062 Dresden, Germany*

*Received May 28, 2003. In Final Form: August 11, 2003*

Photo-cross-linkable temperature and pH-responsive polymers based on *N*-isopropylacrylamide and 2-(dimethylmaleimido)-*N*-ethyl-acrylamide were synthesized and spin-coated to produce uniform thin films of cross-linked, responsive hydrogels. Surface plasmon resonance and optical waveguide spectroscopy were used to determine the effect on the volume-phase transition when these materials are confined to a thin film. The film thicknesses ranged from 10 nm to 2.5 $\mu$m, and the volume-phase transition temperature and swelling ratio of the films fell into two overlapping regimes separated by at least one critical thickness. In the thick-film regime, greater than 100−760 nm, depending on the cross-linking density, ionizable comonomer concentration, and reference state, the films exhibited two transition temperatures. This can be explained by the stress imposed on the hydrogel as it swells perpendicular to the substrate. In the thin-film regime, less than 270−440 nm, depending on cross-linking density, the presence of a fixed substrate also limited the collapse of the gel at temperatures above the volume-phase transition temperature. Nonequilibrium chain conformations resulting from the spin-coating process may explain this effect. Two different mechanisms for constraint are likely in the thin- and thick-film regimes, and existing models for the anisotropic swelling of hydrogel layers were used to explain these trends. The spin-coated hydrogel layers were also compared to dip-coated and free-radical polymerized hydrogel layers to provide additional insight to the constraint mechanism. The elastic modulus of the hydrogel layers was measured with atomic force microcopy. The modulus in the swollen state was a function of both the cross-linking density and the ionizable comonomer concentration and ranged from 4.48 to 26.6 kPa. The modulus in the collapsed state was primarily a function of the cross-linking density and ranged from 466 to 1540 kPa. The effect of the ionizable comonomer concentration on the modulus also suggests the presence of non-Gaussian chain conformations in the swollen network.

## Introduction

The characteristics of responsive polymers and hydrogels have been studied extensively for applications such as chemomechanical actuators, drug delivery, and separation systems,[1−5] and a wide range of techniques have been used to make films, membranes, and responsive surfaces from these materials.[6−12] The resulting surfaces can change their contact angle,[6] affinity for different compounds in chromatographic separations,[13] and adhesion[14,15] and frictional properties[16] in response to an external stimulus. One of the most intensively studied polymers in this field is poly(*N*-isopropylacrylamide) (PNIPAAm), which exhibits a temperature-induced collapse from an extended coil to a globular structure in water upon heating above 32 °C.[3] This leads to a sudden decrease in the degree of swelling of cross-linked PNIPAAm gels. The volume-phase transition has been described theoretically as resulting from a balance between mixing free energy, rubber elasticity free energy, and, in the case of ionizable comonomers, the osmotic contribution of the counterions.[17−21]

The same approach has been extended to include gels of different shapes and anisotropic swelling in both one and two dimensions,[22] but anisotropic swelling is usually related to the gel being placed under stress or being confined in some way. The swelling of hydrogel layers and patterns has been shown to be highly anisotropic, and the volume change is confined to one dimension,

* To whom correspondence should be addressed. E-mail: dirk.kuckling@chemie.tu-dresden.de (D.K.); curt.frank@stanford.edu (C.W.F.).

† Stanford University.

‡ Technische Universität Dresden.

(1) Gehrke, S. H. *Adv. Polym. Sci.* **1993**, *110*, 81−144.
(2) Osada, Y.; Gong, J. P. *Adv. Mater. (Weinheim, Ger.)* **1998**, *10*, 827−837.
(3) Schild, H. G. *Prog. Polym. Sci.* **1992**, *17*, 163−249.
(4) Freitas, R. F. S.; Cussler, E. L. *Chem. Eng. Sci.* **1987**, *42*, 97−103.
(5) Dong, L. C.; Hoffman, A. S. *J. Controlled Release* **1990**, *13*, 21−31.
(6) Takei, Y. G.; Aoki, T.; Sanui, K.; Ogata, N.; Sakurai, Y.; Okano, T. *Macromolecules* **1994**, *27*, 6163−6166.
(7) Pan, Y. V.; Wesley, R. A.; Luginbuhl, R.; Denton, D. D.; Ratner, B. D. *Biomacromolecules* **2001**, *2*, 32−36.
(8) Liang, L.; Rieke, P. C.; Fryxell, G. E.; Liu, J.; Engehard, M. H.; Alford, K. L. *J. Phys. Chem. B* **2000**, *104*, 11667−11673.
(9) Ivanova, I. G.; Kuckling, D.; Adler, H.-J. P.; Wolff, T.; Arndt, K.-F. *Des. Monomers Polym.* **2000**, *3*, 447−462.
(10) Trank, S. J.; Cussler, E. L. *Chem. Eng. Sci.* **1987**, *42*, 381.
(11) Zhou, S. Q.; Wu, C. *Macromolecules* **1996**, *29*, 4998−5001.
(12) Yakushiji, T.; Sakai, K.; Kikuchi, A.; Aoyagi, T.; Sakurai, Y.; Okano, T. *Langmuir* **1998**, *14*, 4657−4662.
(13) Kikuchi, A.; Okano, T. *Prog. Polym. Sci.* **2002**, *27*, 1165−1193.
(14) Ito, Y.; Chen, G. P.; Guan, Y. Q.; Imanishi, Y. *Langmuir* **1997**, *13* (3), 2756−2759.
(15) Morra, M.; Cassinelli, C. *Polym. Prepr.* **1995**, *36*, 55−56.
(16) Gong, J. P.; Kagata, G.; Osada, Y. *Macromol. Symp.* **2000**, *159*, 215−220.
(17) Shibayama, M.; Tanaka, T. *Adv. Polym. Sci.* **1993**, *109*, 1−62.
(18) Dusek, K.; Prins, W. *Adv. Polym. Sci.* **1969**, *6*, 1−102.
(19) Hooper, H. H.; Baker, J. P.; Blanch, H. W.; Prausnitz, J. M. *Macromolecules* **1990**, *23*, 1096−1104.
(20) Ilavsky, M. *Macromolecules* **1982**, *15*, 782−788.
(21) Flory, P. J. *Principles of Polymer Chemistry*; Cornell University Press: Ithaca, NY, 1953.
(22) Onuki, A. *Adv. Polym. Sci.* **1993**, *109*, 63−121.

10.1021/la030217h CCC: $25.00 
Published on Web 12/16/2003

perpendicular to the substrate.[23−25] For high degrees of swelling and film thicknesses on the order of 100 $\mu$m, this can cause the gel to buckle, creating a pattern on the gel surface.[26] The volume-phase transition has also been confined to two dimensions by placing gel rods under uniaxial strain,[27−29] and the applied stress has been shown to affect the transition temperature.[28,30,31] Gel phase coexistence is frequently present in gels under constraint[32] but has also been observed for temperature- and electro-responsive hydrogels swelling in three dimensions with no constraint.[33−35]

The change in the transition temperature with applied stress often complicates the mechanical measurements of responsive hydrogels near the transition temperature,[31] but the mechanical properties of bulk hydrogels have been measured by indentation,[36] simple tension and compression,[20,37] scattering,[38] and dynamic mechanical analysis.[39] In the swollen state, the modulus is a function of the ionic content and cross-linking density as the resulting swelling ratio and network chain concentration change. Such behavior can be described by rubber elasticity theory of a swollen cross-linked network.[21] Ionic content does not affect the modulus in the collapsed state,[20] which is determined primarily by the cross-linking density.[40] The gel modulus is also a function of a reference state where the distribution of the polymer chain conformations is Gaussian.[21] The swelling is assumed to be isotropic, and the reference state is usually assumed to be where the cross-links are formed. The modulus generally decreases with increasing ionic content, but for strong polyelectrolytes and gels with high ionic content,[41] the modulus begins to increase with increased ionic content as a result of the aggregation and condensation of ions at high ionic compositions[42,43] or as a result of non-Gaussian chain conformations at high degrees of swelling.[36]

Atomic force microscopy (AFM) has been widely used for imaging and mechanical measurements of soft materials.[44−47] Force−distance curves can also be generated, with the resulting indentation of the cantilever under a given load being used to calculate the surface elastic modulus,[48] but the resulting elastic modulus values tend to be high relative to the bulk material properties. AFM studies of responsive hydrogels range from single-chain experiments[49] to tribology[50] and modulus[51,52] measurements, and AFM imaging has revealed domains on the submicrometer length scale that are related to inhomogeneous gel network structures.[53−55]

When comparing the swelling behavior and mechanical properties of gel layers, it is also important to consider the effects of different cross-linking conditions. Hydrogel layers cross-linked in the dry state are always swollen relative to their reference state, while those that are cross-linked in solution can be either swollen or collapsed relative to their reference state. Furthermore, when polymer films are cast from solvent, the polymers have a tendency to align in the plane of the film,[56−60] and the chain orientation can be varied through different methods of film preparation.[61,62] Although the anisotropy and residual stress from the solvent-coating process can be removed by annealing,[56,63−65] the presence of a substrate can substantially alter the properties of the film. These effects are usually limited to films on the order of the polymer radius of gyration[61,64] but have been seen for film thicknesses on the order of micrometers.[63,66]

We have studied photo-cross-linked PNIPAAm hydrogel layers prepared by spin coating, and these materials have shown a film thickness dependence of both the transition temperature and the refractive index in the collapsed state.[25,32] The swelling behavior fell into two regimes separated by at least one "critical thickness." This does not refer to a critical phenomenon in the thermodynamic sense; rather, this terminology refers to a film thickness above or below at which a particular effect is seen. The refractive index and film thickness could be measured simultaneously by using a combination of surface plasmon

(23) Revzin, A.; Russell, R. J.; Yadavalli, V. K.; Koh, W. G.; Deister, C.; Hile, D. D.; Mellott, M. B.; Pishko, M. V. *Langmuir* **2001**, *17*, 5440−5447.
(24) Hoffmann, J.; Plotner, M.; Kuckling, D.; Fischer, W. J. *Sens. Actuators, A* **1999**, *77*, 139−144.
(25) Kuckling, D.; Harmon, M. E.; Frank, C. W. *Macromolecules* **2002**, *35*, 6377−6383.
(26) Tanaka, T.; Sun, S. T.; Hirokawa, Y.; Katayama, S.; Kucera, J.; Hirose, Y.; Amiya, T. *Nature (London)* **1987**, *325*, 796−798.
(27) Suzuki, A.; Kojima, S. *J. Chem. Phys.* **1994**, *101*, 10003−10007.
(28) Suzuki, A.; Ishii, T. *J. Chem. Phys.* **1999**, *110*, 2289−2296.
(29) Suzuki, A.; Sanda, K.; Omori, Y. *J. Chem. Phys.* **1997**, *107*, 5179−5185.
(30) Suzuki, A. *Adv. Polym. Sci.* **1993**, *110*, 199−240.
(31) Hirotsu, S. *J. Chem. Phys.* **1991**, *94*, 3949−3957.
(32) Harmon, M. E.; Kuckling, D.; Frank, C. W. *Macromolecules* **2003**, *36*, 162−172.
(33) Bai, G.; Suzuki, A. *J. Chem. Phys.* **1999**, *111*, 10338−10346.
(34) Hirotsu, S. *Adv. Polym. Sci.* **1993**, *110*, 1−26.
(35) Tanaka, T.; Nishio, I.; Sun, S. T.; Uenonishio, S. *Science (Washington, D.C.)* **1982**, *218*, 467−469.
(36) Dubrovskii, S. A.; Rakova, G. V. *Macromolecules* **1997**, *30*, 7478−7486.
(37) Ikehata, A.; Ushiki, H. *Polymer* **2002**, *43*, 2089−2094.
(38) Schosseler, F.; Ilmain, F.; Candau, S. J. *Macromolecules* **1991**, *24*, 225−234.
(39) Tong, Z.; Liu, X. X. *Macromolecules* **1993**, *26*, 4964−4966.
(40) Shibayama, M.; Morimoto, M.; Nomura, S. *Macromolecules* **1994**, *27*, 5060−5066.
(41) Okay, O.; Durmaz, S. *Polymer* **2002**, *43*, 1215−1221.
(42) Khokhlov, A. R.; Kramarenko, E. Y. *Macromol. Theory Simul.* **1994**, *3*, 45−59.
(43) Zeldovich, K. B.; Khokhlov, A. R. *Macromolecules* **1999**, *32*, 3488−3494.
(44) Domke, J.; Radmacher, M. *Langmuir* **1998**, *14*, 3320−3325.
(45) Schonherr, H.; Wiyatno, W.; Pople, J.; Frank, C. W.; Fuller, G. G.; Gast, A. P.; Waymouth, R. M. *Macromolecules* **2002**, *35*, 2654−2666.
(46) Jena, B. P., Hörber, J. K. H., Eds. *Atomic Force Microscopy in Cell Biology*; Academic Press: San Diego, 2002.
(47) Tsukruk, V. V.; Gorbunov, V. V.; Huang, Z.; Chizhik, S. A. *Polym. Int.* **2000**, *49*, 441−444.
(48) Van Landingham, M. R.; Villarrubia, J. S.; Guthrie, W. F.; Meyers, G. F. *Macromol. Symp.* **2001**, *167*, 15−43.
(49) Zhang, W. K.; Zou, S.; Wang, C.; Zhang, X. *J. Phys. Chem. B* **2000**, *104*, 10258−10264.
(50) Matzelle, T. R.; Herkt-Bruns, C.; Heinrich, L. A.; Kruse, N. *Surf. Sci.* **2000**, *454*, 1010−1015.
(51) Matzelle, T. R.; Ivanov, D. A.; Landwehr, D.; Heinrich, L. A.; Herkt-Bruns, C.; Reichelt, R.; Kruse, N. *J. Phys. Chem. B* **2002**, *106*, 2861−2866.
(52) Harmon, M. E.; Kuckling, D.; Frank, C. W. *Langmuir* **2003**, *19*, 10660−10665.
(53) Suzuki, A.; Yamazaki, M.; Kobiki, Y. *J. Chem. Phys.* **1996**, *104*, 1751−1757.
(54) Suzuki, A.; Yamazaki, M.; Kobiki, Y.; Suzuki, H. *Macromolecules* **1997**, *30*, 2350−2354.
(55) Kobiki, Y.; Suzuki, A. *Int. J. Adhes. Adhes.* **1999**, *19*, 411−416.
(56) Frank, C. W.; Rao, V.; Despotopoulou, M. M.; Pease, R. F. W.; Hinsberg, W. D.; Miller, R. D.; Rabolt, J. F. *Science (Washington, D.C.)* **1996**, *273*, 912−915.
(57) Prest, W. M.; Luca, D. J. *J. Appl. Phys.* **1979**, *50*, 6067−6071.
(58) Prest, W. M.; Luca, D. J. *J. Appl. Phys.* **1980**, *51*, 5170−5174.
(59) Cohen, Y.; Reich, S. *J. Polym. Sci., Part B: Polym. Phys.* **1981**, *19*, 599−608.
(60) Hall, D. B.; Underhill, P.; Torkelson, J. M. *Polym. Eng. Sci.* **1998**, *38*, 2039−2045.
(61) Prucker, O.; Christian, S.; Bock, H.; Ruhe, J.; Frank, C. W.; Knoll, W. *ACS Symposium Series* **1998**, *695*, 233−249.
(62) Kurabayashi, K.; Goodson, K. E. *J. Appl. Phys.* **1999**, *86*, 1925−1931.
(63) Frank, B.; Gast, A. P.; Russell, T. P.; Brown, H. R.; Hawker, C. *Macromolecules* **1996**, *29*, 6531−6534.
(64) Reiter, G. *Europhys. Lett.* **1993**, *23*, 579−584.
(65) Takahashi, N.; Yoon, D. Y.; Parrish, W. *Macromolecules* **1984**, *17*, 2583−2588.
(66) Ree, M.; Chu, C. W.; Goldberg, M. J. *J. Appl. Phys.* **1994**, *75*, 1410−1419.

**Chart 1. Monomers Used for Polymer Synthesis**

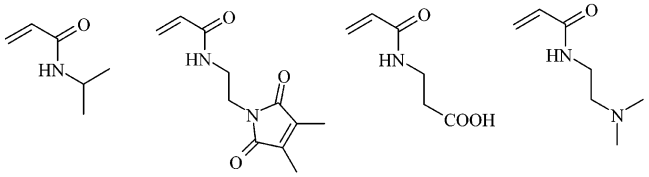


resonance (SPR) and optical waveguide spectroscopy (OWS), and the volume-phase transition was detected in response to both temperature and pH.[25,32] Optical microscopy has been used to study the effects of film thickness on thicker hydrogel layers prepared by free-radical polymerization,[67] and we have also used SPR to study the gel−substrate interface for these materials.[68] A comparison of these results indicates that there is an effect of the film thickness, cross-linking density, degree of ionization, and method of film preparation. This paper will explore these systems in greater detail and determine how each of these parameters affects the volume-phase transition in constrained hydrogel layers. By comparing several different systems on the basis of the same responsive polymers, the relative effects can provide additional insight to the mechanism of constraint in responsive hydrogel layers.

## Experimental Section

**Materials.** *N*-Isopropylacrylamide (NIPAAm, Aldrich) was purified by recrystallization from hexane and dried in a vacuum. 2,2′-Azobis(isobutyronitrile) (AIBN) was recrystallized from methanol. Dioxane, tetrahydrofuran, and diethyl ether were distilled over potassium hydroxide. All other reagents were of analytical grade and were used as received. The 2-(dimethylmaleimido)-*N*-ethyl-acrylamide (DMIAAm),[69] 3-acryloylaminopropionic acid (AAmPA),[70] and *N*-(2-(dimethylamino)-ethyl)-acrylamide (DMAAAm)[71] monomers were prepared according to the literature.

**Synthesis of the Photo-Cross-Linkable Polymers.** The PNIPAAm copolymers were obtained by free-radical polymerization of NIPAAm as the central component, DMIAAm as the photo-cross-linkable component, and acidic AAmPA or basic DMAAAm as the ionizable component (see Chart 1). The reaction was initiated with AIBN in dioxane, and the details of this synthesis have been published previously.[25,32] The composition of the copolymers could be determined from $^1$H NMR spectra recorded from polymer solutions in acetone-$d_6$ and by acid−base titration. The molecular weight ($M_w$) and the molecular weight distribution (polydispersity $M_w/M_n$) of the copolymers were determined by gel-permeation chromatography with a Waters instrument equipped with UV and IR detectors and using Waters' "Ultrastyragel" columns. The samples were measured at 30 °C in chloroform containing 0.1 vol % triethylamine as the mobile phase with a flow rate of 1 mL/min.

The copolymers are referred to as NIPAAm followed by the percentage feed composition of the DMIAAm chromophore (for example, NIPAAm2). All terpolymers have approximately 5% DMIAAm content, and the notation used for the terpolymers consists of the acidic or basic comonomer followed by the percentage feed composition of that comonomer (for example, AAmPA5). The monomers selected have similar structures and should, therefore, have comparable reactivities. The name of each sample and its corresponding composition and molecular weight can be found in Table 1.

**Table 1. Characterization of Linear Polymers**

| sample | DMIAAm [mol %] | AAmPA [mol %] | DMAAAm [mol %] | $M_w$ [g/mol] |
|---|---|---|---|---|
| NIPAAm2 | 2.4 | | | 148 000 |
| NIPAAm5 | 4.5 | | | 83 500 |
| NIPAAm10 | 9.2 | | | 36 100 |
| AAmPA2 | 4.3 | 2.5 | | 85 100 |
| AAmPA5 | 5.3 | 4.9 | | 114 000 |
| AAmPA10 | 4.7 | 10.1 | | 134 000 |
| DMAAAm2 | 5.0 | | 1.2 | 78 800 |
| DMAAAm5 | 4.3 | | 3.9 | 102 000 |
| DMAAAm10 | 5.9 | | 9.8 | 77 700 |

**Responsive Hydrogel Layers.** Two different techniques were used to prepare responsive hydrogel layers. Photo-cross-linked layers were cross-linked in the dry state while free-radical polymerized layers were cross-linked in the swollen state.

*Photo-Cross-Linked Linear Polymers.* Photo-cross-linked polymer films were prepared by spin coating or dip coating of an SPR substrate from a cyclohexanone solution containing different wt % polymer, ranging from 0.1 to 20 wt %, and 2 wt % thioxanthone sensitizer with respect to the polymer. The resulting film thicknesses varied with the viscosity of the polymer solution and ranged from 10 nm to 2.5 $\mu$m. The SPR substrates were LaSFN9 glass slides coated with a 50-nm gold film, which was deposited by evaporation with an Edwards 306 Autocoater. The films were dried under vacuum and cross-linked by UV irradiation, using a 75-W high-pressure Hg lamp at a wavelength $\lambda > 300$ nm, for at least 60 min. The kinetics of the photo-cross-linking reaction have been reported previously,[25] and this results in complete conversion of the dimethylmaleimide group. The procedure resulted in hydrogel layers that were physisorbed to the substrate, but a separate set of experiments used SPR substrates that had been functionalized with an adhesion promoter, thioacetic acid 3-dimethylmaleimido propyl ester, designed to form a covalent bond between the gold substrate and the hydrogel layer. The synthesis of the adhesion promoter is described in the following, along with the surface modification of the SPR substrates.

*Free-Radical Polymerization.* Responsive hydrogel layers were also formed from the free-radical polymerization of NIPAAm, sodium acrylate (SA, ionizable comonomer), and *N*,*N*′-methylenebisacrylamide (BIS, cross-linker), initiated by ammonium persulfate (APS) and *N*,*N*,*N*′,*N*′-tetramethylethylenediamine (TEMED). A sol−gel process was used to produce a 20-nm silica film on the gold substrate.[68,72] This process is compatible with SPR measurements and produces films that are stable under a wide range of pressure, pH, and temperature values. The silica layer was treated with $\gamma$-methacryloxypropyltrimethoxysilane as a surface coupling agent, and thin films of the NIPAAm gel were cast using Teflon spacers according to the procedure of Zheng and co-workers.[73] This approach also produced a covalent bond between the hydrogel layer and the substrate. The pregel solution was prepared by dissolving NIPAAm (700−630 mM), SA (0−70 mM), BIS (3.5−15 mM), and TEMED (20 $\mu$L) in 3 mL of Milli-Q water and purging with nitrogen. A total of 60 $\mu$L of a 40 mg/mL solution of APS in Milli-Q water was added to initiate the polymerization. The total network concentration (sum of SA and NIPAAm) was kept constant at 700 mM. The thickness of the resulting gel films was 3 $\mu$m in the dry state, as determined by profilometry.[68]

**Adhesion Promoter for Gold Surfaces.** Thioacetic acid 3-dimethylmaleimido propyl ester (see Scheme 1) will form a covalent bond between the gold substrate and the dimethylmaleimido group of the cross-linked network. A similar adhesion promoter has also been designed to form a covalent bond between the cross-linked network and silicon substrates.[74]

(67) Suzuki, A.; Wu, X. R.; Kuroda, M.; Ishiyama, E.; Kanama, D. *Jpn. J. Appl. Phys., Part 1* **2003**, *42*, 564−569.
(68) Harmon, M. E.; Jakob, T. A. M.; Knoll, W.; Frank, C. W. *Macromolecules* **2002**, *35*, 5999−6004.
(69) Ling, L.; Habicher, W. D.; Kuckling, D.; Adler, H. J. *Des. Monomers Polym.* **1999**, *2*, 351−358.
(70) Kuckling, D.; Adler, H. J. P.; Arndt, K. F.; Ling, L.; Habicher, W. D. *Macromol. Chem. Phys.* **2000**, *201*, 273−280.
(71) Kuckling, D.; Adler, H. J. P.; Arndt, K. F.; Ling, L.; Habicher, W. D. *Macromol. Symp.* **1999**, *145*, 65−74.
(72) Kambhampati, D. K.; Jakob, T. A. M.; Robertson, J. W.; Cai, M.; Pemberton, J. E.; Knoll, W. *Langmuir* **2001**, *17*, 1169−1175.
(73) Zheng, J. J.; Odake, T.; Kitamori, T.; Sawada, T. *Anal. Chem.* **1999**, *71*, 5003−5008.
(74) Kuckling, D.; Hoffmann, J.; Plötner, M.; Ferse, D.; Kretschmer, K.; Adler, H.-J. P.; Arndt, K.-F.; Reichelt, R. *Polymer* **2003**, *44*, 4455−4462.

**Scheme 1. Synthesis of the Adhesion Promoter**

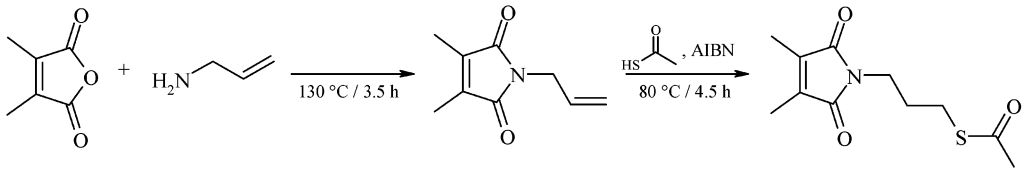


**1** **2**

*Synthesis of Thioacetic Acid 3-Dimethylmaleimido Propyl Ester (**2**).* 1-Allyl-dimethylmaleimide (**1**) was prepared according to the literature.[75] Thioacetic acid 3-dimethylmaleimido propyl ester (**2**) was prepared by adding 1.727 g (22.7 mmol) of thioacetic acid to a stirred solution of 2.50 g (15.1 mmol) of **1** in 15 mL of chloroform. A total of 147 mg (0.9 mmol) AIBN was added to this mixture, and the solution was heated to 80 °C for 4.5 h. The mixture was cooled to room temperature followed by the addition of 30 mL of saturated sodium bicarbonate solution. The aqueous phase was extracted twice with 45 mL of petroleum ether each. The organic phase was washed twice with 45 mL of saline solution each and dried over magnesium sulfate. After removal of the solvent in a vacuum, the crude product was purified by column chromatography on silica gel (ethyl acetate/hexane, 2:8, $R_f$ = 0.3) to yield 2.9 g (79%) of **2** as a viscous liquid.

$^1$H NMR ($CDCl_3$): $\delta$ 1.82 (tt, $^3J$ = 7.2 Hz, $^3J$ = 6.8 Hz, 2H, $CH_2$), 1.92 (s, 6H, $CH_3$), 2.28 (s, 3H, $CH_3$), 2.75 (t, $^3J$ = 7.2 Hz, 2H, S—$CH_2$), 3.45 (t, $^3J$ = 6.8 Hz, 2H, N—$CH_2$). $^{13}$C NMR ($CDCl_3$): $\delta$ 8.62 ($2CH_3$), 26.23 (S—$CH_2$), 28.65 (N—$CH_2$), 30.51 ($CH_3$), 36.66 ($CH_2$), 137.12 (C═C), 172.08 (2C═O), 195.41 (S—C═O). IR (KBr), $\nu$ (cm$^{-1}$): 2932 (C—H), 1768 and 1707 (C═O), ca. 1690 (O═C—S). Elem anal. Calcd. for $C_{11}H_{15}NO_3S$: C, 54.75; H, 6.26; N, 5.81; S, 13.28. Found: C, 54.62; H, 6.44; N, 6.20; S, 13.01.

The $^1$H NMR spectra were recorded on a Bruker DRX-500. IR spectra were measured on a Unicam RS 1000 Fourier transform infrared (FTIR) instrument. Elemental analysis was carried out on a Carlo Erba CHNS-O EA 1108 elemental analyzer.

*Surface Modification*. The SPR substrates were submerged in a 1 mM solution of thioacetic acid 3-dimethylmaleimido propyl ester in 200 proof ethanol, rinsed with ethanol, and dried with a nitrogen stream, and the samples were then spin-coated and cross-linked as described previously. The presence of the adhesion promoter on the gold substrate could be detected by FTIR at grazing incidence due to an increase of the C—H vibration band at around 3000 cm$^{-1}$. The binding of the protected thiol[76] on the gold substrate could also be detected with SPR. Finally, the change in the contact angle and the reduced lateral swelling of the resulting hydrogel layers were taken as confirmation of the surface functionalization.

**SPR and OWS.** The refractive index and film thickness of the hydrogel layers were measured simultaneously, using a combination of SPR and OWS in the Kretschmann configuration.[77] The data analysis used a two-layer model, which has been described previously,[32] and the resulting swelling ratio and transition temperature values are in good agreement with optical microscopy and differential scanning calorimetry measurements on the same materials.[25] This technique can be used for hydrogel layers with a dry film thickness ranging from 100 nm to 3 $\mu$m. For films thinner than 100 nm, SPR can be used to determine the transition temperature, but the film thickness and refractive index cannot be calculated.[32]

**Swelling Experiments.** The swelling behavior of the photo-cross-linked gel films was observed as a function of temperature in DI water from a Milli-Q system. The samples were placed in a flow-through cell that was connected to a peristaltic pump, and the temperature of the solute was controlled externally by a temperature-controlled bath. The temperature inside the cell was measured with a thermocouple and was accurate within 0.1 °C. The response time of the gels is on the order of seconds; this is much faster than the time scale of the temperature change in the flow cell, which is several minutes. The equilibration time between each angular scan ranged from 10 to 25 min, and this was verified in the SPR kinetic mode, in which the reflected intensity at a fixed angle is monitored as a function of time. The initial equilibration step also served to leach out the sensitizer prior to collecting data.

OWS can be used to study anisotropy in thin films,[77] and although there are indications of anisotropy in the dry films, the swollen gel layers have a refractive index that is isotropic.[32] Thus, the SPR and OWS data were used to calculate the refractive index and swelling ratio of the hydrogel layers as a function of the temperature. These data were fit to a sigmoidal curve, and the inflection point of the curve was defined as the transition temperature. Cylindrical bulk gels were also synthesized, and the transition temperature was defined by tracking the gel diameter, using the procedure of Tanaka and co-workers.[17,78] There is an inherent difference between gel cylinders and slabs as the transition temperature is affected by the energy of the curved hydrogel surface,[79] but the comparison of cylindrical bulk hydrogels and hydrogel layers has been used to study the effects of constraint in these materials.[68]

**Hydrogel Mechanical Properties.** The mechanical properties of the hydrogel layers were measured using AFM. Standard AFM cantilevers and cantilevers modified with a 5-$\mu$m silica sphere were used to generate force—distance curves according to the procedure of Matzelle and co-workers.[51] A fluid cell was used in combination with a custom-built heating stage comprising a Peltier element and water cooling to maintain the piezo-electric stage at a constant temperature. Standard AFM cantilevers were used for dry films and colloidal cantilevers were used for measurements in the liquid cell. The indentation of the cantilever under a given load was fit to the Hertz model for indentation of a sphere (colloidal silica) or cone (standard cantilever) on an elastic solid and used to calculate the elastic modulus of the hydrogel layer.[51] The modulus generated by indentation measurements is known to be a function of the film thickness and indentation.[44,48] To minimize these effects, the modulus was measured as a function of the indentation and dry film thickness. The modulus values were found to be consistent for dry film thicknesses greater than 500 nm with indentations of less than 20% of the film thickness, and films on the order of 500 nm for the dry film thickness were, therefore, used for the modulus measurements presented here.

## Results

**Models for Anisotropic Gel Swelling.** Anisotropic swelling of hydrogels has been modeled and used to describe the length scales of patterns that appear on the gel surface as the gel begins to buckle at high degrees of swelling.[26,80,81] The gel is cross-linked in some reference state (see Figure 1) and is under lateral compression, increasing with distance away from the substrate, when it is swollen relative to the reference state. Conversely, the gel is under elongation when it is collapsed relative to the reference state. A gel layer that is cross-linked in the dry state is always under compression while swollen,

(75) Kuckling, D.; Hoffmann, J.; Plötner, M.; Ferse, D.; Kretschmer, K.; Adler, H.-J. P.; Arndt, K.-F.; Reichelt, R. *Polymer*, in press.
(76) Ming, M.; Chen, Y.; Katz, A. *Langmuir* **2002**, *18*, 2413—2420.
(77) Knoll, W. *Annu. Rev. Phys. Chem.* **1998**, *49*, 569—638.
(78) Hirokawa, Y.; Tanaka, T. *J. Chem. Phys.* **1984**, *81*, 6379—6380.
(79) Hirotsu, S. *Macromolecules* **1992**, *25*, 4445—4447.
(80) Onuki, A. *J. Phys. Soc. Jpn.* **1988**, *57*, 1868—1871.
(81) Sekimoto, K.; Kawasaki, K. *J. Phys. Soc. Jpn.* **1987**, *56*, 2997—3000.

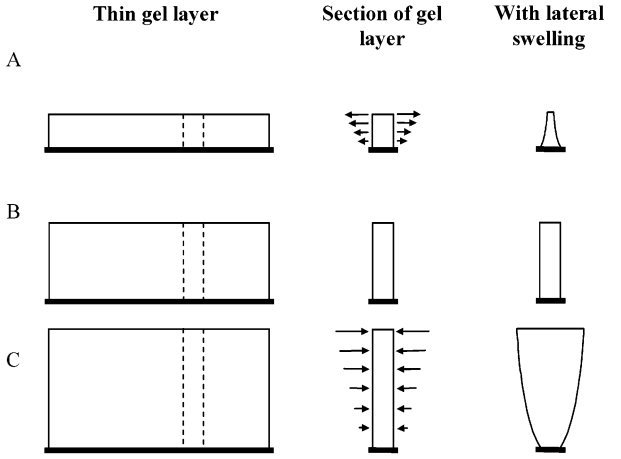


**Figure 1.** The hydrogel layer is cross-linked in some reference state (B), and the gel at the substrate remains in this reference state. The elastic energy of the network acts as compression when the gel layer is swollen (C) relative to the reference state and as elongation when the gel layer is collapsed (A) relative to the reference state. The compression or elongation increases monotonically and is greatest at the free surface of the gel. Our measurements are for infinitely wide films, but the exact shape of the gel with lateral swelling depends on both the film thickness and the aspect ratio of the gel layer.

but a gel layer that is cross-linked in the swollen state can be under compression or elongation, depending on the degree of swelling. Specifically, the degree of swelling near the transition temperature is difficult to predict, and although recent models have been able to predict the degree of swelling in the swollen and collapsed states, they fail to describe the discontinuity of the resulting volume-phase transition.[67] The model shown in Figure 1 has only been applied to gel swelling and has not been used to describe the collapse of a gel layer during the volume-phase transition. However, we will use this more qualitative framework to explain the trends in the refractive index and swelling ratio for the anisotropic swelling of gel layers.

**Effect of Film Thickness.** Photo-cross-linked PNIPAAm hydrogel layers prepared by spin coating have shown a film thickness dependence of both the refractive index in the collapsed state and the transition temperature.[25,32] The swelling behavior fell into two regimes, separated by a critical thickness, and an example of this effect is shown in Figure 2 for the NIPAAm5 sample. The refractive index of the hydrogel layer is low at low temperatures, where the gel is hydrophilic and water-swollen, and high at high temperatures, where the gel is hydrophobic, collapsed, and contains little water. We will present data for the refractive index of the hydrogel layers, and the corresponding swelling ratio is inversely related to the refractive index. Therefore, with increasing temperature, the refractive index increases, and the swelling ratio decreases and approaches one when the gel is fully collapsed. The solid lines are from sigmoidal fits in Origin, using the following empirical expression:

$$n = n(\text{collapsed}) + \frac{n(\text{swollen}) - n(\text{collapsed})}{1 + \exp\left(\frac{T - T_c}{\Delta T_c}\right)}$$

where $T_c$ is the transition temperature at the inflection point of the curve, $n$(swollen) is the refractive index at low temperatures, $n$(collapsed) is the refractive index at high temperatures, and $\Delta T_c$ is a measure of the temperature

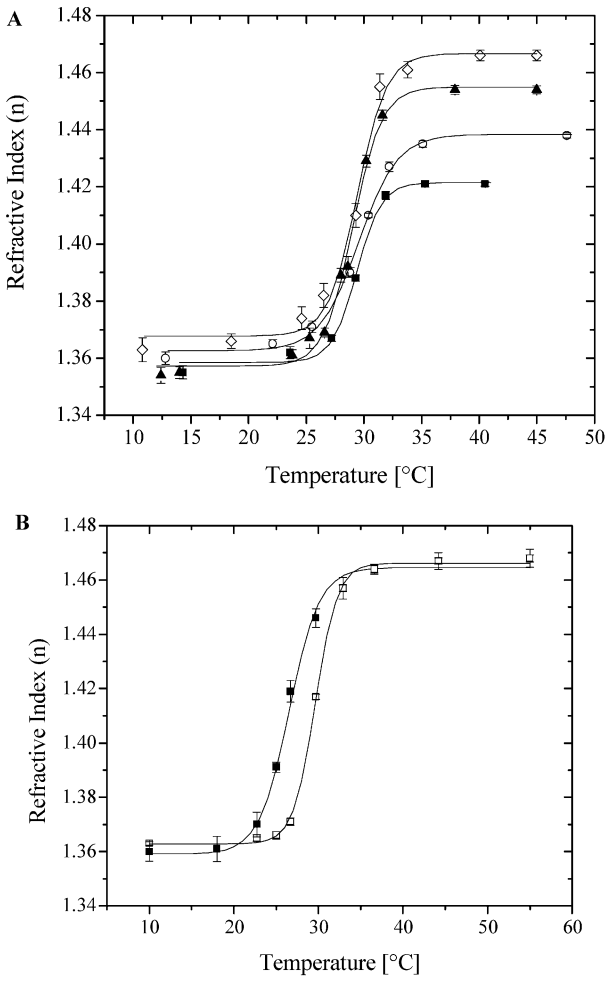


**Figure 2.** The refractive index of the photo-cross-linked NIPAAm5 sample is shown as a function of the temperature in the DI water for different thicknesses (total thickness of dry film) of physisorbed films. (A) In the thin-film regime, the refractive index in the collapsed state decreases as a function of film thickness (◇, 577 nm; ▲, 299 nm; ○, 196 nm; and ■, 136 nm). (B) In the thick-film regime, the transition temperature of the gel far from the substrate (■, layer 2) is lower than that of the gel−substrate interface (□, layer 1), and the transition temperature of layer 2 is a function of the film thickness. The film shown is 2270-nm thick, and the transition temperature of layer 2 is 3 °C lower than that of layer 1.

range over which the transition takes place. The thin-film regime is shown in Figure 2A, and both $T_c$ and $n$(swollen) appear to be independent of the film thickness. The 577-nm film has the same value of $n$(collapsed) as the thicker films, but as the film thickness decreases, $n$(collapsed) begins to decrease. The corresponding swelling ratio in the collapsed state ranges from 1.18 for the 577-nm film to 1.79 for the 136-nm film, and the decrease in the refractive index is, therefore, an indication that the films are unable to fully collapse at temperatures above the transition temperature. The thick-film regime is shown in Figure 2B, and both $n$(swollen) and $n$(collapsed) are independent of the film thickness. The transition temperature of the substrate gel layer (1) is the same as that for the thinner films, but the transition temperature of the free-surface gel layer (2) is lower than that of layer 1.

The transition temperature of layer 2 has been shown to decrease above some critical film thickness,[32] and this effect was measured as a function of the cross-linking

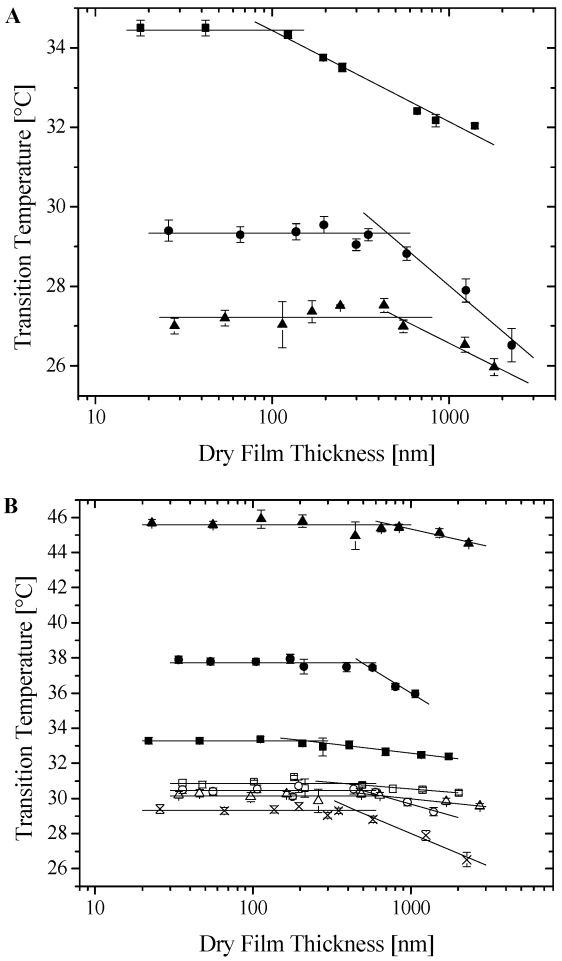


**Figure 3.** The transition temperature of layer 2 is shown as a function of the film thickness for physisorbed films with different (A) cross-linking densities (■, NIPAAm2; ●, NIPAAm5; and ▲, NIPAAm10) and (B) ionizable comonomer compositions (×, NIPAAm5; □, AAmPA2; ○, AAmPA5; △, AAmPA10; ■, DMAAAm2; ●, DMAAAm5; and ▲, DMAAAm10). The critical film thicknesses (see Table 2) are defined by the intercept of the linear fits above and below the apparent transition.

**Table 2. Intercepts of Linear Fits from Figures 3, 4, and 7**

| | *h*(critical) [nm] | | |
|---|---|---|---|
| sample | *n*(collapsed) | $T_c$(gold substrate) | $T_c$(adhesion promoter) |
| NIPAAm2 | 270 | 100 | 90 |
| NIPAAm5 | 350 | 450 | 420 |
| NIPAAm10 | 440 | 520 | |
| AAmPA2 | 280 | 370 | |
| AAmPA5 | 280 | 500 | |
| AAmPA10 | 280 | 670 | |
| DMAAAm2 | 280 | 220 | |
| DMAAAm5 | 280 | 490 | 400 |
| DMAAAm10 | 280 | 760 | |

density and ionizable comonomer concentration (see Figure 3). The transition temperature decreases with increasing cross-linking density because the cross-linking chromophore makes the network more hydrophobic. By contrast, the transition temperature increases with increasing ionizable comonomer concentration because the ionized groups make the network more hydrophilic and increase the osmotic pressure inside the gel. The critical thickness (see Table 2) increases with increasing cross-linking density and increasing ionizable comonomer

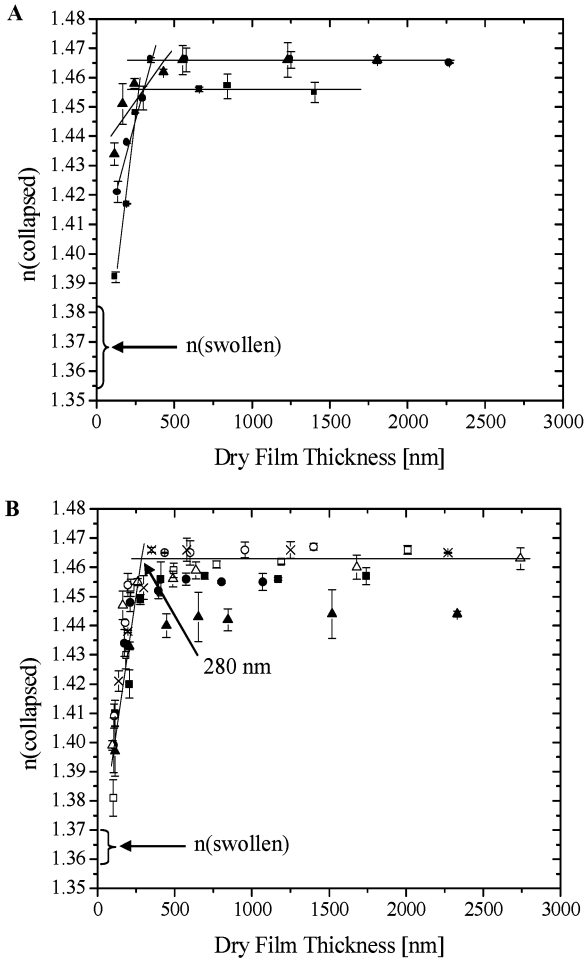


**Figure 4.** The refractive index in the collapsed state is shown as a function of the film thickness for physisorbed films with different (A) cross-linking densities (■, NIPAAm2; ●, NIPAAm5; and ▲, NIPAAm10) and (B) ionizable comonomer compositions (×, NIPAAm5; □, AAmPA2; ○, AAmPA5; △, AAmPA10; ■, DMAAAm2; ●, DMAAAm5; and ▲, DMAAAm10). The refractive index in the swollen state changes as a function of the cross-linking density, as shown by the arrows. The critical film thicknesses (see Table 2) are defined by the intercept of the linear fits above and below the apparent transition. For films with similar cross-linking densities but different ionic compositions, the refractive indices below 280 nm appear to fall on a single curve.

concentration, but the effect appears to be greater for the basic DMAAAm comonomer than for the acidic AAmPA monomer.

The refractive index in the collapsed state decreases below some critical film thickness, with the effects of the cross-linking density and ionizable comonomer concentration on *n*(collapsed) shown in Figure 4. The refractive index in the collapsed state approaches the refractive index for the swollen state, as indicated by the arrows. This suggests that at some film thickness the films would be completely unable to collapse, but it is not clear whether this extrapolation is meaningful. For samples with similar cross-linking densities and different ionic compositions, all the data appear to fall on a single curve below a critical thickness of 280 nm (see Figure 4B). However, samples with different cross-linking densities have different critical thicknesses (see Table 2) and different slopes at thicknesses below the critical film thickness (see Figure 4A).

**Effect of the Gel Modulus.** The modulus of the hydrogel layers was measured using AFM force−distance curves. The modulus ($G$) of a swollen network can be

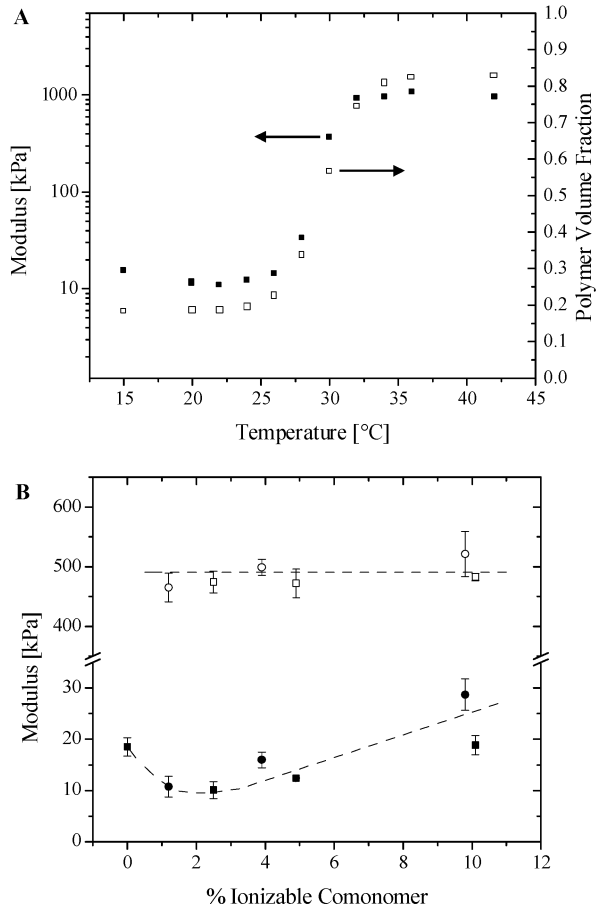


**Figure 5.** (A) Modulus (■) and volume fraction (□) of a physisorbed NIPAAm5 hydrogel layer as a function of the temperature in DI water. (B) Modulus of the physisorbed hydrogel layer as a function of the AAmPA (□/■) and DMAAAm (○/●) comonomer concentrations. The values shown are for the collapsed (open symbols, 42 °C) and swollen (solid symbols, 15 °C) states. The dissociation constant is different for AAmPA and DMAAm, and the lines are drawn to guide the eye as an average for the two ionizable comonomers.

described by rubber elasticity theory and should increase with increasing polymer volume fraction.[21] The volume fraction of polymer can be calculated from the refractive index, and the gel modulus does increase with increasing polymer fraction, as shown in Figure 5A. A direct comparison between the rubber elasticity theory and the modulus values measured here can give additional insight to the hydrogel morphology, and this will be published in a subsequent paper along with AFM images of the hydrogel surface.[52]

The transition temperature can also be estimated by plotting the modulus as a function of the temperature and is similar to that determined with SPR and OWS. Figure 5A shows modulus values from AFM experiments and polymer volume fraction values from SPR and OWS experiments, and the transition temperature from both sets of experiments is around 30 °C. The modulus of each sample in air and in water at temperatures above (42 °C) and below (15 °C) the transition temperature is given in Table 3. The modulus in the swollen state is a function of both the cross-linking density and the degree of ionization, while the modulus in the collapsed state appears to be independent of the ionic composition (see Figure 5B). The modulus in the collapsed state is between that for the swollen state and that for the dry state (see Table 3), which is consistent with the collapsed gel network

**Table 3. Gel Film Modulus Values**

| | modulus [kPa] | | |
|---|---|---|---|
| sample | swollen[a] | collapsed[b] | dry[c] |
| NIPAAm2 | 4.48 | 486 | 1850 |
| NIPAAm5 | 12.7 | 914 | 1940 |
| NIPAAm10 | 26.6 | 1540 | 1950 |
| AAmPA2 | 10.1 | 474 | 1940 |
| AAmPA5 | 12.4 | 472 | 1960 |
| AAmPA10 | 16.9 | 483 | 1840 |
| DMAAAm2 | 10.8 | 466 | 1970 |
| DMAAAm5 | 18.0 | 499 | 1910 |

[a] In DI water at 15 °C. [b] In DI water at 42 °C. [c] In dry air at room temperature.

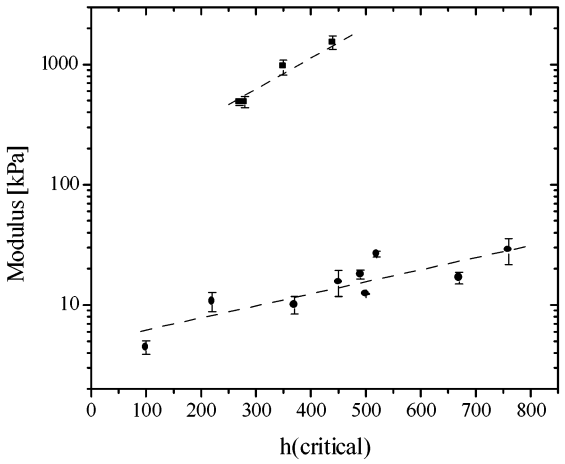


**Figure 6.** The correlation between the modulus and *h*(critical) for physisorbed hydrogel layers is shown, with *h*(critical) increasing as the modulus increases. The values shown are the modulus in the collapsed state (■, 42 °C) as a function of the critical film thickness for *n*(collapsed) and the modulus in the swollen state (●, 15 °C) as a function of the critical film thickness for $T_c$. The lines are drawn to guide the eye.

containing a small amount of water. The modulus in both the swollen and the collapsed states also correlates well with the critical thicknesses, as shown in Figure 6. The plot shows a comparison of the critical thicknesses in Table 2 and the modulus values for the corresponding samples in Table 3. The modulus and film thickness data fall onto two curves, indicating that these two parameters are closely related. It is expected that the effect of the fixed substrate should be felt farther from the substrate for gels with a higher modulus, and this is also shown in Figure 6 as *h*(critical) increases with increasing modulus.

**Effect of the Reference State.** We have modified the gel−substrate interface to verify that the film thickness effects are not related to the gold substrate surface energy or inhibition of the cross-linking reaction through coupling between the gold layer and the chromophores.[32] However, the data in Figure 6 indicate that these effects are a function of the gel modulus. The modulus of a swollen cross-linked network is a function of the reference state, which is determined by the cross-linking conditions.[21,36] For a hydrogel layer, this can be probed by forming cross-links between the substrate and the network and by varying the conditions when the cross-links are formed.

*Adhesion Promoter.* The photo-cross-linked hydrogel layers represented by the data in Figures 2−6 were physisorbed to the substrate, and the resulting swelling was highly anisotropic.[25] However, there is some finite lateral swelling, and an adhesion promoter (see Scheme 1) was used to further reduce the lateral swelling. The use of an adhesion promoter may deplete the number of cross-links near the gel−substrate interface because some

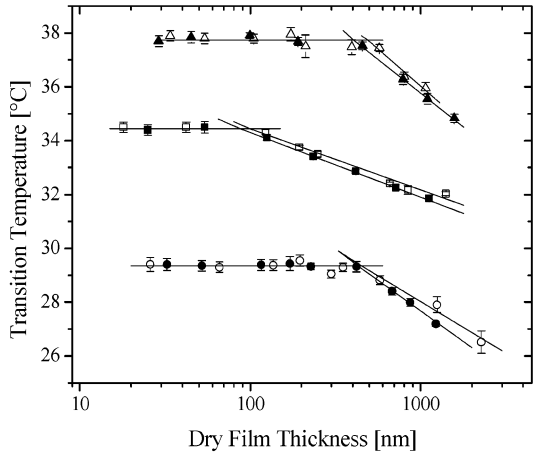


**Figure 7.** An adhesion promoter is used to form a covalent bond between the gel and the substrate. The effect of this adhesion promoter on the transition temperature of the hydrogel layers is shown for samples with varying cross-linking densities and ionizable comonomer compositions (□/■, NIPAAm2; ○/●, NIPAAm5; and △/▲, AAmPA5). The solid symbols are for gels that are physisorbed to a gold substrate, and the open symbols are for a gold substrate functionalized with the adhesion promoter.

of the DMIAAm groups will react with the substrate. However, this region is on the order of the mesh size of the gel and should be negligible as compared to the film thickness effects seen here. Measurements with the NIPAAm2, NIPAAm5, and DMAAAm5 samples were repeated on gold substrates modified with the adhesion promoter. The refractive index in the swollen and collapsed states was not affected by the adhesion promoter (data not shown), but the transition temperatures were slightly lower for each of the samples (see Figure 7). The resulting critical thicknesses were also lower, as shown in Table 2.

*Free-Radical Polymerization.* It is difficult to control the degree of lateral swelling for these hydrogel layers, but the reference state can be varied by changing the cross-linking conditions. Free-radical polymerized gels, which are under compression when swollen and extension when collapsed, are, therefore, an interesting contrast to the photo-cross-linked systems. These materials are also easily formed in the bulk, allowing a comparison between the hydrogel layers and the bulk hydrogels. Hydrogel layers were compared to cylindrical bulk gels, and while the hydrogel layers are covalently bound to the substrate and have negligible lateral swelling, the bulk hydrogels are able to swell isotropically. Both sets of samples have a single transition temperature that varies as a function of the cross-linking density and ionizable comonomer concentration (see Figure 8), and the differences between the two sets of data will be addressed in Discussion.

*Coating Technique.* The effect of the reference state can also be probed by keeping the cross-linking density constant and changing the solvent-coating process. When polymer films are cast from solvent, the polymers have a tendency to align in the plane of the film.[56−60] It is likely that the spin coating followed by vacuum drying and photo-cross-linking causes these chain conformations to be trapped in the gel network. These effects are a function of the polymer radius of gyration ($R_g$), and the data for the refractive index in the collapsed state is very similar when the data is rescaled as a function of the dry film thickness/$R_g$. This is most prominent when comparing the data for gels with different cross-linking densities, as shown by comparing Figures 9A and 4A. Samples with similar cross-linking densities also have similar molecular weights, as

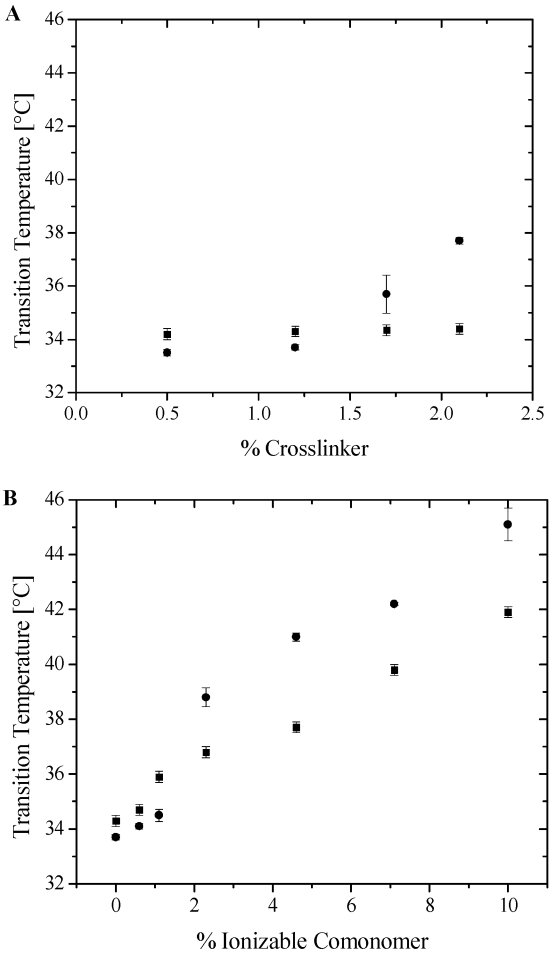


**Figure 8.** The transition temperature for hydrogel layers (●) and bulk hydrogels (■) prepared by free-radical polymerization. The substrate is functionalized with a surface coupling agent so that a covalent bond is formed between the gel and the substrate, and the resulting hydrogel layers have a single transition temperature. (A) The transition temperature varies as a function of the cross-linker (BIS) concentration for samples with 0% SA and 700 mM total network concentration. (B) The transition temperature varies as a function of the ionizable comonomer (SA) concentration for samples with 1.2% BIS and 700 mM total network concentration.

shown in Table 1, and the critical thicknesses are 13.2 ± 2.4 times the calculated diameter ($2R_g$) of the corresponding polymer chains.[82]

The preferential alignment of the polymer chains in the plane of the substrate can usually be reduced by annealing. However, for these particular materials the annealing process causes the thioxanthone sensitizer to phase separate, and the resulting films cannot be photo-cross-linked. Other photo-cross-linking schemes that do not include a sensitizer have been used with PNIPAAm polymers,[83,84] and these systems may be useful for further studies. However, NIPAAm5 samples can also be prepared by dip coating, which is known to produce some anisotropy, but this should be less than the corresponding spin-coated samples.[85] A comparison of these two sets of data is shown in Figure 9B, where the refractive index of the hydrogel

(82) Kubota, K.; Fujishige, S.; Ando, I. *Polym. J.* **1990**, *22*, 15−20.
(83) Kuckling, D.; Adler, H. J. P.; Arndt, K. F.; Hoffmann, J.; Plotner, M.; Wolff, T. *Polym. Adv. Technol.* **1999**, *10*, 345−352.
(84) Kang, M. S.; Gupta, V. K. *J. Phys. Chem. B* **2002**, *106*, 4127−4132.
(85) Lin, L.; Bidstrup, S. A. *J. Appl. Polym. Sci.* **1993**, *49*, 1277−1289.

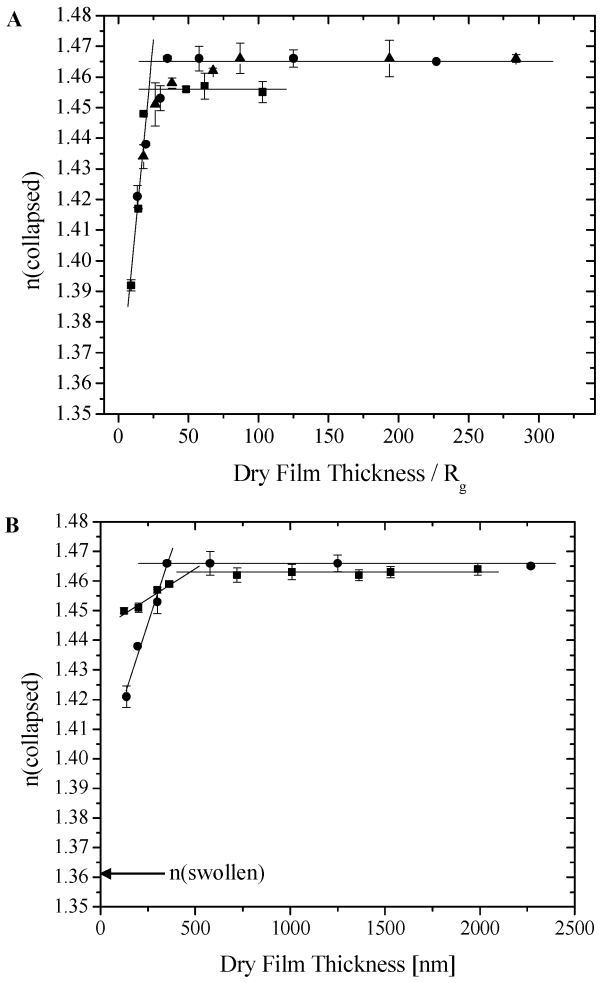


**Figure 9.** (A) The data in Figure 4A is rescaled as a function of the dry film thickness/$R_g$ (■, NIPAAm2; ●, NIPAAm5; and ▲, NIPAAm10). (B) The effect of the solvent-coating technique on hydrogel layers prepared from the NIPAAm5 linear polymer. The hydrogel layers are all physisorbed to the substrate, but the refractive index in the collapsed state changes when the samples are prepared by spin coating (●) and dip coating (■). The refractive index in the swollen state is constant, as shown by the arrow.

layer in the collapsed state is clearly affected by the change in the solvent-coating process. The coating technique does not affect the transition temperature of these hydrogel layers (data not shown).

## Discussion

**Transition Temperature of Hydrogel Layers.** The transition temperature of bulk PNIPAAm gels has been shown to increase with elongation[28] and decrease with compression,[30,31] which is consistent with the photo-cross-linked hydrogels being cross-linked in the dry state and being under compression as they swell perpendicular to the substrate. The compression is greater farther from the substrate (see Figure 1), and the corresponding transition temperature is also lower (see layer 2 in Figure 2B). Thus, layer 2 could be interpreted as the region of the gel where this compression is great enough to affect the transition temperature. It is not clear from these measurements over what length scale the transition temperature continues to decrease, but at some point the gels should begin to buckle in response to the lateral stresses.[26] This has been observed with the optical microscopy of photo-cross-linked gels that have dry film thicknesses on the order of 10 $\mu$m,[24] which is beyond the practical limit of the SPR and OWS measurements presented here, and the film thickness at which these surface patterns begin to appear is not known. The lateral compression should also be a function of the osmotic pressure exerted by the counterions and the ability of the network chains to deform in response to the stress.[26,81] The concentration of DMAAAm appears to have a stronger effect on $h$(critical) for the transition temperature than the corresponding concentration of AAmPA (see Table 2). This is consistent with previous measurements, which indicate that DMAAAm dissociates more strongly in DI water than AAmPA,[32] and DMAAAm should, therefore, have a stronger osmotic contribution to the gel swelling and the resulting lateral compression.

The most important difference between the data for the photo-cross-linked and the free-radical polymerized hydrogel layers is that the free-radical polymerized hydrogel layers exhibit a single transition temperature (see Figure 8), independent of the film thickness,[68] while the photo-cross-linked hydrogel layers exhibit one or two transition temperatures, depending on film thickness (see Figure 2). The transition temperature depends on the compression or elongation at some intermediate degree of swelling close to the transition temperature. Gels that are cross-linked in the dry state are under compression as they swell, and the relative degrees of the cross-linking density and ionizable comonomers are clearly related to the degree of lateral compression. However, when the hydrogel layers are cross-linked in the swollen state, the degree of swelling near the transition temperature can be significantly different from that when the cross-links are formed.[86] Therefore, it is not always clear whether the gel is under compression or elongation near the transition temperature. On the basis of the data for the hydrogel layers prepared by free-radical polymerization (see Figure 8), it appears that this is a function of the degree of cross-linking and the concentration of ionizable comonomers. At low cross-linking densities and concentrations of ionizable comonomer, the transition temperatures are lower than in the bulk, indicating that the gel layers are under compression. At some intermediate cross-linking density and ionizable comonomer concentration, there is a crossover, and at higher concentrations, the resulting hydrogel layers are apparently under elongation near the transition temperature.

**Hydrogel Morphology.** Hydrogels are known to have an inhomogeneous porous or spongy structure in the swollen and collapsed states, with a submicrometer length scale.[51,53,55,87] AFM imaging and mechanical measurements can be achieved by using a standard AFM cantilever with the appropriate spring constant[47] or a cantilever modified with a silica sphere.[51,52] When measuring the modulus of dry hydrogel films in air, the colloid-modified AFM cantilevers produced little or no indentation, and using standard AFM cantilevers improved the reproducibility of these measurements. When measuring the modulus of swollen and collapsed films in water, AFM cantilevers modified with a silica sphere gave more consistent measurements. This is likely due to the inhomogeneous structure of the gel surface, and when using a probe that is larger than the length scale of these structures, the resulting modulus is an average value for the hydrogel layer.

(86) Hirotsu, S.; Hirokawa, Y.; Tanaka, T. *J. Chem. Phys.* **1987**, *87*, 1392−1395.
(87) Hirokawa, Y.; Jinnai, H.; Nishikawa, Y.; Okamoto, T.; Hashimoto, T. *Macromolecules* **1999**, *32*, 7093−7099.

The increase in the modulus as a function of ionizable comonomer concentration is shown in Figure 5B and is an indication of the aggregation and condensation of ions at high ionic compositions[42,43] or non-Gaussian chain conformations at high degrees of swelling.[36] DMAAAm is known to dissociate more strongly than AAmPA in DI water,[32] and this is consistent with the more rapid increase in the modulus for the DMAAAm data. Here, these effects are seen at lower degrees of swelling and lower concentrations of ionizable comonomers than previous reports of hydrogel mechanical properties. The increase appears around a 2% ionizable comonomer concentration (see Figure 5B), and it is unlikely that there would be significant aggregation or condensation of ions at this degree of ionization. However, the appearance of non-Gaussian chain conformations at relatively low ionizable comonomer concentrations can be explained by the reference states of the different hydrogel materials. Previous reports of the mechanical properties of hydrogels have been for gels cross-linked in the swollen state, and with low ionizable comonomer concentrations, these gels are still relatively close to their reference state.[42,43] The photo-cross-linked hydrogels shown here are swollen four to eight times their dry film thicknesses, which should be sufficient to introduce non-Gaussian chain conformations. In this highly swollen regime, a small increase in the ionizable comonomer concentration would, therefore, produce an increase in the hydrogel modulus.

**Refractive Index of Hydrogel Layers.** We have shown that three different variables correlate with *n*(collapsed) as a function of the film thickness: the cross-linking density (see Figure 4A), modulus (see Figure 6), and polymer molecular weight (see Table 1). The cross-linking density affects individual network chain mobility and also affects the resulting network modulus, which should in turn affect the energy required for the gel to collapse. The polymers with higher DMIAAm content result in networks with higher cross-linking density, but these polymers also have lower molecular weights (see Table 1). The polymer molecular weight affects the elongation of the chains during the spin-coating process, and samples prepared by spin coating were, therefore, compared to samples prepared by a dip-coating process (see Figure 9B). Stress-induced orientation during spin coating seems to be the most convincing argument to explain the behavior of the photo-cross-linked hydrogel layers in the thin-film regime. The critical thickness ranges from 90 to 760 nm, which is much larger than the polymer radius of gyration. However, because the gel network is cross-linked, the effects of the substrate can more easily translate to effects away from the substrate.

**Mechanism of Constraint.** We have described these hydrogel layers as being under constraint, and the resulting effects fall into two distinct regimes, separated by a critical thickness. There appear to be two different mechanisms that determine the effect of the film thickness on the refractive index in the collapsed state in the thin-film regime and on the transition temperature in the thick-film regime. The use of an adhesion promoter to form a covalent bond between the substrate and the hydrogel layer affects the transition temperature (see Figure 7) but does not affect the refractive index of the gel layer in the swollen or collapsed states. Conversely, preparing the hydrogel layers by dip coating affects the refractive index in the collapsed state (see Figure 9) but does not affect the transition temperature.

The critical film thicknesses for the two regimes (see Table 2) are also affected by different variables. The effect of the film thickness on the transition temperature varies with the modulus and the gel reference state, and the transition temperature is determined by the stress distribution in the gel as it swells perpendicular to the substrate. The trends seen here are consistent with existing theory, but it should be noted that the reference state is not the only difference between the photo-cross-linked and free-radical polymerized systems. Because the distribution of the cross-linked chromophores is determined by the free-radical polymerization of the linear DMIAAm copolymers, the photo-cross-linked hydrogel layers are likely to have a high concentration of dangling chain ends. There is also a different chain orientation due to the spin-coating process, and the detailed effects of this network morphology on the anisotropic swelling of the resulting hydrogel layers are unknown. The effect of the film thickness on *n*(collapsed) varies with the molecular weight of the polymer, and this is determined by non-equilibrium chain conformations in the dry state, resulting from the spin-coating process. This makes it unfavorable for the network chains to approach this conformation as the hydrogel layer becomes hydrophobic at temperatures above the transition temperature. This mechanism could prevent the gel from fully collapsing, but a more detailed study of the solvent-coating conditions will be necessary to fully understand this effect.

## Conclusion

The volume-phase transition of constrained hydrogel layers was studied by SPR and OWS as a function of the film thickness, cross-linking density, ionizable comonomer concentration, and reference state. This technique has been applied previously, but a study of the relative magnitudes of these effects gave additional insight to the mechanism of the anisotropic swelling of responsive hydrogels. The swelling behavior is affected by the nonequilibrium chain conformations resulting from the spin-coating process as well as the stress distribution in the gel layer. This varies as a function of both the gel modulus, measured by AFM force−distance curves, and the gel reference state, which can be varied by the method of preparation. The swelling behavior and mechanical properties of the photo-cross-linked hydrogel layers can be compared to previous reports of free-radical polymerized hydrogels by considering the effects of the different reference states. Finally, these measurements can be compared to theoretical models for hydrogel swelling, and this can be used to describe the hydrogel morphology and to explain the trends seen as a function of the film thickness.

**Acknowledgment.** The DFG is gratefully acknowledged for financial support within the SFB 287 “Reactive Polymers”. D.K. is thankful to the Max Kade Foundation for a scholarship. The work was also supported by a NSF Graduate Research Fellowship (M.E.H.), the Center on Polymer Interfaces and Macromolecular Assemblies (CPIMA), which was sponsored by the NSF-MRSEC program under DMR 9808677, and the NSF XYZ-on-a-chip program under DMR 9980799.

LA030217H